Journal of Rehabilitation Research and
Development Vol. 38 No. 1, January/February 2001
Pages 123–128

SLO radiant power and brightness

Rolf W. Nygaard, PhD and Ronald A. Schuchard, PhD
Department of Ophthalmology, University of Missouri-KC, Kansas City, MO 64108; VA Rehab R&D Center and Emory University School of Medicine, Decatur, GA 30322

Abstract—Available output in the Scanning Laser Ophthalmoscope (SLO) may be expressed as radiant power at the beam pivot (SLO exit pupil), in units of microwatts (μW). This power corresponds to dimensions of brightness (like luminance and retinal illuminance) and to a range of related measures (like cd/m^2, lm/m^2, and the troland value) in both free and Maxwellian views. We demonstrate that the conversion factor power/troland=1.26*10^{-3} μW and 3.15*10^{-4} μW for SLO nominal visual angles 40˚ and 20˚, respectively. The factor permits measured SLO power to be expressed in units of brightness and (inversely) brightnesses of everyday objects to be expressed in units of SLO power. Examples of both conversions are given. Reference to the literature demonstrates the importance of expressing SLO power in brightness terms common to everyday activities and to visual function-testing instruments besides the SLO.

Key words: *calibration, laser, ophthalmoscopy, SLO.*

INTRODUCTION

The Scanning Laser Ophthalmoscope (SLO; reference 1) has been used for perimetry, fixation, pursuit, acuity, and contrast sensitivity evaluations where precise control of visible stimulus presentations on the retina is essential. Vision research studies and clinical services that make use of the SLO, however, often fail to report the actual brightness of their testing stimuli in terms that can be immediately related to brightness evaluated in the optical perspectives of free and Maxwellian views. Here, we will consider the relationship between SLO power (usually measured in watts or the more convenient microwatts) and brightness (both at the source and detector). From this, we shall derive the numerical factors that permit conversion between these two dimensions.

BACKGROUND

Let us take a moment to review some preliminary concepts. Refer to **Figure 1**. First, "free view" is the optical perspective of the everyday human observer or, more precisely, "[image formation] with minimal accessory optics" (2). "Maxwellian view" is the optical perspective of many clinical instruments (including the SLO) in which the illumination source and natural pupil are conjugate (3).

Photopic "efficacy" is the maximum luminous effectiveness of radiant power (lumens/watt) in the light-adapted human observer. Photopic "efficiency" is relative efficacy normalized to the observer's maximum spectral

This material is based on work supported in part by VA Rehabilitation, Research, & Development Service grant #C838-RA1, the Eye Foundation of Kansas City, and Children's Mercy Hospital.

Address all correspondence and requests for reprints to: Rolf W. Nygaard, PhD, Department of Vision Sciences, Children's Mercy Hospital, 2401 Gilham Road, Kansas City, MO 64108; email: rnygaard@cmh.edu.

Journal of Rehabilitation Research and Development Vol. 38 No. 1 2001

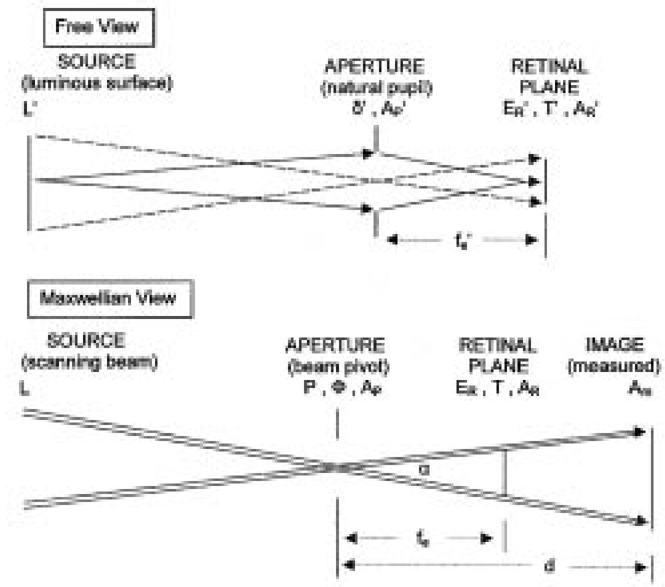

Figure 1.
Two optical geometries. Top (free view): power (solid lines) from a uniform source of luminance (L') is apertured by the natural pupil of diameter δ' and area A_P'. Refracted rays travel f_e' and fall focused on A_R', circumscribed by chief image rays (dashed lines). This produces uniform retinal illuminance (E_R') with troland value (T'). Bottom (SLO-Maxwellian view): power from a scanning laser beam of uniform luminance (L) creates an optical pupil at its pivot of area A_P ($<A_P'$) which apertures all source power (P*, Φ). The unrefracted beam (proceding in a path similar to chief image rays of free view) travels $f_e = f_e'$, scanning through angle α and falling on A_R. This produces uniform retinal illuminance (E_R) with troland value (T). A_m is measured area of illumination a distance d from the pivot and $A_R = A_m * f_e^2/d^2$.

sensitivity. Together, photopic efficacy and efficiency map radiant power into photopic power. In both free and Maxwellian views, source brightness is often scaled in the dimension of "luminance" (photopic power density at the source). Detector brightness, on the other hand, is often scaled in the dimension of "retinal illuminance" (photopic power density at the retinal detector). Retinal illuminance proportionalized to a standard gives the "troland value." Dividing corresponding radiant power and troland values gives the relationship between source (e.g., SLO) power and detector (e.g., retinal) brightness.

In SLO visible mode, a beam of radiant flux from a monochromatic (λ=633 nm HeNe laser) source rapidly scans the retinal surface (at roughly 192,000 pixel locations), producing an image varying in 256 grayscale increments (from 0 to 255). One full-field scan is completed in approximately 30 ms, within the human visual system's energy-integration period. (Image formation by an SLO is photometrically indistinguishable from image formation by a nonscanning Maxwellian system.) During the scan, beam movement "pivots" about a fixed locus positioned near the plane of the eye's natural pupil (more precisely, at its posterior nodal point). This "beam pivot," the SLO exit pupil, is the Maxwellian source image at the natural pupil. The SLO radiant power can be measured at the beam pivot by laser-power meters that integrate flux over meter-detector area.

GENERAL METHODS

Integrating over wavelength (λ) the product of radiant power (P{λ}) in microwatts (μW; as mentioned above, this unit is more convenient to the SLO user than is the watt) with photopic efficacy at 555 nm (K_m) and photopic efficiency (V{λ}), we get photopic power (Φ) in lumens (lm).

$\Phi = K_m(lm/\mu W) * {}_{\lambda} [P\{\lambda\}(\mu W) * V\{\lambda\}]\, d\lambda$ (**Equation 1a**) (4).

Assuming constant P and V over a unit λ,

$\Phi = K_m(lm/\mu W) * P(\mu W) * V$ (**Equation 1b**).

Inserting standard values ($K^m = 683*10^{-6}$ lm/μW and V=0.239 at 633 nm) (5) gives photopic power for the SLO (using a HeNe laser),

$\Phi = 163*10^{-6}(lm/\mu W) * P(\mu W)$ (**Equation 1c**).

Let Φ be uniformly distributed over a simulated retinal area (A_R) scaled in meter² (m²). By the term "simulated" we mean that A_R is a plane area in empty (i.e., lossless, homogeneous, and isotropic) space, positioned normal to and at a standard emmetropic distance (f_e) from the beam pivot. (Indeed, use of the term f_e acknowledges disregard for individual variation in intraocular path length.) Then, retinal illuminance is

$E_R = \Phi(lm)/A_R(m^2)$ (**Equation 1d**) (6).

Substituting **Equations 1c** into **1d** and solving for P,

$P = E_R(lm/m^2) * A_R(m^2)/[163*10^{-6}(lm/\mu W)] = E_R * A_R * 6.13*10^3$ (μW) (**Equation 1e**).

A conventional brightness relationship in free (primed units) and Maxwellian (unprimed units) views is $E_R' = L' * A_P'pr/(f_e')^2$ and $E_R = L * A_P/(f_e)^2$ (**Equation 2a**) (7),

where L' and L are source luminances (cd/m²); A_P' and A_P are limiting pupil apertures (m²); f_e' and f_e are standard emmetropic distances ($16.67*10^{-3}$ m). Relative to the unit troland (0.00359 lm/m²), the troland values (T′, T) of any E_R' and E_R are

$T'=E_R'(\mathrm{lm/m^2})/0.00359(\mathrm{lm/m^2})$ and $T=E_R(\mathrm{lm/m^2})/0.00359(\mathrm{lm/m^2})$ (**Equation 2b**) (8).

The unit troland (0.00359 lm/m²) is obtained from **Equation 2a** with L′, L=1 cd/m²; A_P', $A_P=10^{-6}$ m²; f_e', $f_e=16.67$ mm.

Dividing **Equation 1e** by **Equation 2b** at $E_R'=E_R$ (equal brightness in both views),

P/T' (μW/td) = P/T (μW/td) = $22.0 * A_R$ (**Equation 3**),

for A_R given in m².

Equation 3 allows us to convert SLO power into a commonly used measure of detector brightness, the troland, requiring only a knowledge of A_R. The value is determined in Experiment 1. Then, by using a conventional expression we can convert trolands into a commonly used measure of source brightness, luminance in cd/m². This is done in Experiment 2.

Experiment 1: Methods and Results

To evaluate A_R we measured A_m, the area (in m²) of full and uniform SLO raster scan projected onto a rigidly fixed and flat surface at an angular spread (α) of 20° and 40°. (The α's are manufacturers' specifications that define the angle subtended at the beam pivot by the full raster scan diagonal. Since the SLO display is unconventional (it is trapezoidal with negatively curved sides) we shall refer to it for labeling purposes only.

The projection surface used was the examining room wall, located a known distance (d=2.090 m) from the SLO beam pivot and normal to beam direction. A_m was obtained by first tracing the faint luminous outline of the projected SLO raster scan in an almost completely darkened room and then measuring the included area under full room illumination. A_m was measured in 5 experimental sessions conducted over a period of 50 days. Then, by similar triangles,

$A_R=A_m * f_e^2/d^2$ (**Equation 4**).

Substituting A_R into **Equation 3** gives the number of microwatts per troland for uniform, full-field display. **Table 1** lists values of A_m, A_R, and P/T(μW/td) for each session, session average (Avg), and a. Avg P/T at α=40° is 1.26×10^{-3} μW/td and at α=20° is 3.15×10^{-4} μW/td.

Figure 2 shows **Equation 3** applied to real SLO data. P was measured at 25 equal-interval values (gsv's) of the acousto-optic modulator (aom) with a=20° and beam-attenuating filter 3. Measurement was made with an LM-2 CW laser flux detector head (Coherent Optics, Inc.) positioned at the beam pivot and coupled to a Labmaster digital processor (10-Hz acquisition rate). (Digital coupling to the Labmaster permitted RS-232 computer interface for data acquisition and storage. However, Fieldmaster analog coupling to the LM-2 for manual acquisition is also possible.) We examined a second generation SLO (model #324, Rodenstock, Germany) using full-field, uniform raster scan of the HeNe laser beam. Results were corroborated in a Generation 3 SLO and in an upgraded Generation 1 SLO.

Table 1.

Day	α	A_m (m²)	A_R (m²)	P/T (μW/td)
1	40°	9.22×10^{-1}	5.86×10^{-5}	1.28×10^{-3}
21	40°	9.21×10^{-1}	5.85×10^{-5}	1.28×10^{-3}
24	40°	9.17×10^{-1}	5.83×10^{-5}	1.28×10^{-3}
45	40°	9.32×10^{-1}	5.92×10^{-5}	1.30×10^{-3}
51	40°	8.62×10^{-1}	5.48×10^{-5}	1.20×10^{-3}
Avg	40°	9.10×10^{-1}	5.78×10^{-5}	1.26×10^{-3}
1	20°	2.26×10^{-1}	1.43×10^{-5}	3.14×10^{-4}
21	20°	2.25×10^{-1}	1.43×10^{-5}	3.14×10^{-4}
24	20°	2.31×10^{-1}	1.46×10^{-5}	3.21×10^{-4}
45	20°	2.35×10^{-1}	1.49×10^{-5}	3.27×10^{-4}
51	20°	2.17×10^{-1}	1.38×10^{-5}	3.03×10^{-4}
Avg	20°	2.26×10^{-1}	1.43×10^{-5}	3.15×10^{-4}

Journal of Rehabilitation Research and Development Vol. 38 No. 1 2001

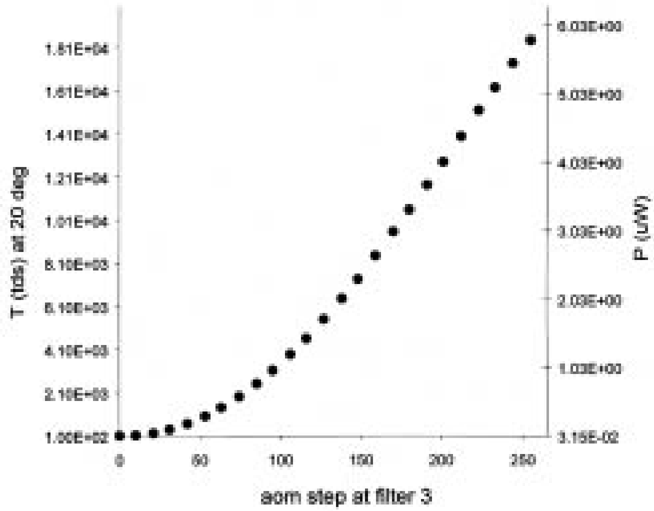

Figure 2.
Actual P (μW) obtained from a SLO (right ordinate). Multiplying P by T/P (td/μW) at α=20º (the inverse of Avg P/T (μW/td) at α=20º in **Table 1**) gives their troland values (left ordinate).

Measured values of P, scaled on the right, range from $3.23*10^{-2}$ μW to 5.81 μW. Multiplying these values by the factor T/P(td/μW)=$3.17*10^{3}$ (the inverse of Avg P/T(μW/td) at α=20˚ in **Table 1**) gives photopically equivalent brightnesses, scaled on the left, ranging from $1.02*10^{2}$ tds to $1.84*10^{4}$ tds.

Experiment 2: Methods and Results

Table 2 lists a sample of 13 luminous surfaces. In each case, L′ (in cd/m²) was measured using a hand-held radiometer with photopic filter attachment (Minolta CS-100). T′ was calculated from the conventional expression

$T'=L'*A_P'$ (td) (**Equation 5a**) (9),

where the product of L′ (in cd/m²) and A_P' (in mm²) is in trolands. **Equation 5a** expresses T′ as E_R' relative to the unit troland. This can be seen as follows. From **Equations 2a** and **2b**,

$T'=[L'(cd/m^2)*A_P'(mm^2)/(f_e'(m))^2]/[1(cd/m^2)*1(mm^2)/(f_e'(m))^2]$ (**Equation 5b**),

which reduces to **Equation 5a**. (The same is true in Maxwellian view.)

A_P' was obtained from the elementary formula

$A_P'=\pi*\delta'^2/4$ (**Equation 5c**),

where δ′ is natural pupil diameter. The value of δ′ was determined from the published empirical expression (using base 10 logs):

$\log[\delta'(mm)]=0.8558 - (4.01*10^{-4})*(\log[L'(cd/m^2)]+8.6)^3$ (**Equation 5d**) (10).

Equation 5d is an empirical relationship relating natural pupil diameter (in mm) with luminance (in cd/m²). It was obtained from pupil sizes of 12 observers viewing 52˚ fields of uniform luminance. The 13 object field sizes listed in **Table 2**, however, were mostly smaller than this. But, except in the 3 brightest cases (red, green, and yellow traffic lights, subtending <1˚) ambient and object luminances were similar, allowing comparison with the literature. In the 3 brightest cases mentioned, ambient luminance exceeded object luminance. But, δ′ was already minimized by the object luminance. Because the greater ambient luminance could have no additional effect, we were justified in using **Equation 5d**.

Finally, P was obtained by multiplying T′ (from **Equation 5a**) into values of P/T′ (from **Equation 3**), given in **Table 1** as Avg P/T (μW/td).

For example, human faces viewed under typical indoor illumination (**Table 2**, row 8) have measured luminances (L′)=110 to 250 cd/m². This corresponds, using **Equation 5a**, to troland values (T′)=470 to 880. From **Table 1**, P/T=$1.26*10-3$ μW/td (α=40˚) and $3.15*10^{-4}$ μW/td (α=20˚). We multiply these into T′ to get the SLO power (P) values of 0.60 to 1.1 μW (α=40˚) and 0.15 to 0.28 μW (α=20˚).

For the nine indoor surfaces measured, luminance and power fields from **Table 2** (columns 2, 4, and 5) were compared. For each α, **Figure 3** plots P(μW) against L′(cd/m²) and fits the scatter with a pair of polynomial trendlines (MS Excel). The positive curvature observed is due to the roughly 50 percent decrease in the value of A_P' as L′ increases from 9 to 340 cd/m².

$P=L'*A_P'$ (td) * P/T′ (μW)/td) (**Equation 6**).

A_P' decreases with increasing L′ so P against L′ is negatively accelerating.

So, now we have a means of converting luminance to trolands, and trolands to photometrically equivalent SLO power (as shown in **Table 2** and **Figure 3**). Use of **Equations 3** and **6** allows SLO power to be related to the brightness of everyday objects, provided we know the retinal area illuminated in SLO view and the pupil-area limiting in free view.

DISCUSSION

Relating SLO power response with brightness gives information valuable to the practitioner in evaluating

Table 2.

Luminous Surface	L′ (cd/m²)	T′ (td)	P(μW) at 40°	P(μW) at 20°
Hallway sign (indoor)	9.0 to 47	(7.3 to 26.) × 10	(9.1 to 32.) × 10^{-2}	(2.2 to 8.1) × 10^{-2}
Carpeting (indoor)	(1.3 to 5.0) × 10	(9.7 to 27.) × 10	(1.2 to 3.4) × 10^{-1}	(3.0 to 8.5) × 10^{-2}
Stairwell (indoor)	(1.8 to 2.5) × 10	(1.2 to 1.6) × 10^2	(1.5 to 2.0) × 10^{-1}	(3.7 to 5.0) × 10^{-2}
Shelved Books (indoor)	(2.5 to 7.5) × 10	(1.6 to 3.6) × 10^2	(2.0 to 4.5) × 10^{-1}	(5.0 to 11) × 10^{-2}
Newspaper (indoor)	(3.0 to 5.1) × 10	(1.8 to 2.7) × 10^2	(2.2 to 3.4) × 10^{-1}	(5.6 to 8.5) × 10^{-2}
TV Screen (indoor)	(4.0 to 8.0) × 10	(2.3 to 3.8) × 10^2	(2.8 to 4.7) × 10^{-1}	(7.2 to 11) × 10^{-2}
Tiled Floor (indoor)	(5.0 to 7.0) × 10	(2.7 to 3.5) × 10^2	(3.4 to 4.4) × 10^{-1}	(8.5 to 11) × 10^{-2}
Human Face (indoor)	(1.1 to 2.5) × 10^2	(4.7 to 8.8) × 10^2	(6.0 to 11.) × 10^{-1}	(1.5 to 2.8) × 10^{-1}
Wristwatch (indoor)	(1.1 to 3.4) × 10^2	(4.6 to 12.) × 10^2	(5.7 to 15.) × 10^{-1}	(1.4 to 3.7) × 10^{-1}
Street Sign (outdoor)	(1.9 to 8.6) × 10^2	(7.0 to 30.) × 10^2	(8.8 to 37.) × 10^{-1}	(2.2 to 9.4) × 10^{-1}
Red Traffic Light (outdoor)	(5.8 to 7.0) × 10^2	(2.0 to 2.4) × 10^3	2.5 to 3.0	(6.3 to 7.5) × 10^{-1}
Green Traffic Light (outdoor)	(1.6 to 1.7) × 10^3	(5.5 to 6.0) × 10^3	6.9 to 7.5	1.7 to 1.9
Yellow Traffic Light (outdoor)	(8.1 to 9.2) × 10^3	(2.8 to 3.2) × 10^4	(3.5 to 4.0) × 10	8.8 to 10

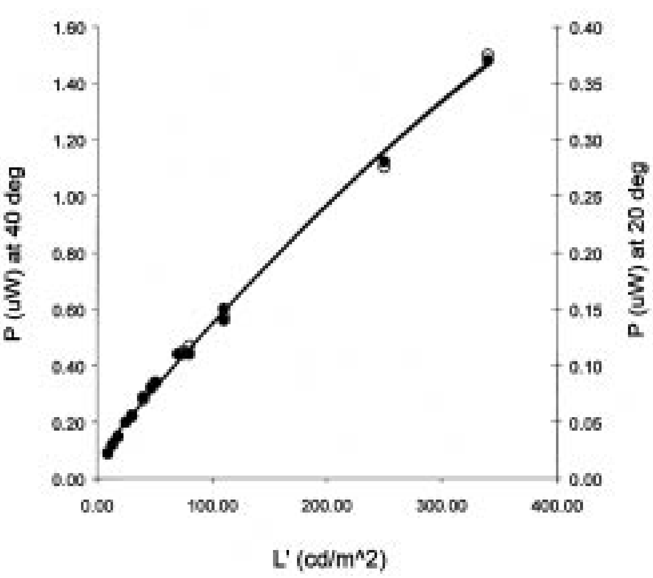

Figure 3.
Plot of the L′ and P fields for the nine indoor surfaces of **Table 2**. Open circles are P (μW) at α=40º; closed circles are P (μW) at α=20º.

therapies for the visually impaired. **Table 2** elaborates the results of studies that use the SLO in clinical situations.

For example, in one study (11) a HeNe beam of 1–2 μW maximum power (α=40˚) was used to map absolute scotomas in a group of patients with macular holes. 1–2 μW at α=40˚ is the SLO power range corresponding to brightnesses of about 793 to 1,580 trolands. (This is seen from **Table 1**: P/T=1.26 $*10^{-3}$ (μW/td), so T/P=793 (td/μW).) From **Table 2**, we see this is typical of human or wristwatch faces viewed indoors and street signs viewed outdoors. Therefore, the absolute scotomas reported were measured at surprisingly low luminances.

Another study (12) described everyday objects whose brightnesses corresponded to measured SLO powers at which patients with a variety of macular disease demonstrated consistent shifts in their preferred retinal locus (PRL) for fixation. Most PRL shifts reported were found to occur at SLO power values (α=40˚) between 0.1 and 1 μW. These values approximate the brightnesses of all **Table 2** objects viewed indoors. The results of that study, therefore, clearly suggest that individuals manifesting similar macular disease may alternate between different PRLs when confronted with common surfaces under typical indoor illumination.

In a study of reading ability in people with impaired visual fields, PRLs were compared using an SLO and a CRT (13). Six patients, who were determined to have central visual field loss from tangent screen examination, had their scotoma locations verified with the SLO. Unfortunately, the authors did not indicate whether the light levels of their tangent screen and SLO were identical. This rendered comparison possible only if the patients had no relative scotomas surrounding the dense scotoma. Moreover, four of the patients had their reading ability compared with an SLO (text background of 38 μW at α=40˚) and a CRT (text background of about 850 cd/m^2). Interpolating in **Table 2** (38 μW at α=40˚ is about 8,700 cd/m^2) reveals that the equivalent luminance in the SLO was about 10 times the reported luminance in the CRT. Therefore, presenting the text with the SLO and CRT might have altered the scotoma boundaries relative to the PRL.

A further study related fixation patterns and reading rates in patients with central scotomas (14). The brightness of the SLO perimetry target was 70,000 trolands. This is equivalent to a very bright outdoor source (exceeding that of a yellow traffic light: see **Table 2**) and, therefore, is appropriate for mapping a dense scotoma. Patient reading rates, however, were determined using a CRT with background luminance of only 181 cd/m^2 (about 680 trolands, interpolating from **Table 2**), a level invisible to many relative scotomas. Thus, the location of scotoma boundaries determined by SLO testing may not have been the same as that under the CRT conditions.

In conclusion, with the factors we have determined that permit conversion between P and T′, T provide a means for relating light levels observed in SLO visual function testing with light levels observed in everyday free viewing and other clinical testing procedures. Forming a bridge between observation in the SLO and the rest of the world, the factors aid in the rehabilitation of persons with vision impairment.

ACKNOWLEDGMENTS

The authors wish to thank Professors S. Burns and V. Lakshminarayanan together with three journal reviewers for their very helpful suggestions on an earlier version of the manuscript.

REFERENCES

1. Webb RH, Hughes GW, Francois CD. Confocal scanning laser ophthalmoscope (SLO). Appl Optics 1987;26:1493.
2. Burns SA, Webb RH. Optical generation of the visual stimulus. In: Bass M, van Stryland EW, Williams DR, et al., (editors). Handbook of optics. New York: McGraw Hill; 1994. 28:2.
3. Burns SA, Webb RH. Optical generation of the visual stimulus. In: Bass M, van Stryland EW, Williams DR, et al., (editors). Handbook of optics. New York: McGraw Hill; 1994. 28:4
4. Wyszecki G, Stiles WS. Color science (2nd ed.) New York: John Wiley & Sons; 1984. p. 256–9, and Equations [3(4.3.2)] and [1(4.3.3)].
5. Wyszecki G, Stiles WS. Color science (2nd ed.) New York: John Wiley & Sons; 1984. p. 256, 258.
6. Burns SA, Webb RH. Optical generation of the visual stimulus. In: Bass M, van Stryland EW, Williams DR, et al., (editors). Handbook of optics. New York: McGraw Hill; 1994. Eqs 5, 11.
7. Burns SA, Webb RH. Optical generation of the visual stimulus. In: Bass M, van Stryland EW, Williams DR, et al., (editors). Handbook of optics. New York: McGraw Hill; 1994. Eq 3 (free view); Burns SA, Webb RH. Optical generation of the visual stimulus. In: Bass M, van Stryland EW, Williams DR, et al., (editors). Handbook of optics. New York: McGraw Hill; 1994. Eq 13; and Wyszecki G, Stiles WS. Color science (2nd ed.) New York: John Wiley & Sons; 1984. p. 481, Eq [7(5.15.1)] (Maxwellian view).
8. Burns SA, Webb RH. Optical generation of the visual stimulus. In: Bass M, van Stryland EW, Williams DR, et al., (editors). Handbook of optics. New York: McGraw Hill; 1994. p. 3.
9. Burns SA, Webb RH. Optical generation of the visual stimulus. In: Bass M, van Stryland EW, Williams DR, et al., (editors). Handbook of optics. New York: McGraw Hill; 1994. p. 3; Wyszecki G, Stiles WS. Color science (2nd ed.) New York: John Wiley & Sons; 1984. p. 102.
10. Wyszecki G, Stiles WS. Color science (2nd ed.) New York: John Wiley & Sons; 1984. p. 106 (Eq 2[2.4.5]).
11. Sjaarda RN, Frank DA, Glaser BM, Thompson JT, Murphy RP. Assessment of vision in idiopathic macular holes with macular microperimetry using the scanning laser opthalmoscope. Ophthalmology 1993;100:1513–8.
12. Lei H, Schuchard R. Using two preferred retinal loci for different lighting conditions in patients with central scotomas. Invest Ophthalmol Vis Sci 1997;38:1812–18.
13. Rubin GS, Turano K. Low vision reading with sequential word presentation. Vis Res 1994;34:1723–33.
14. Sunness JS, Applegate CA, Haselwood D, Rubin GS. Fixation patterns and reading rates in eyes with central scotomas from advanced atrophic age-related macular degeneration and stargardt disease. Ophthalmology 1996;103:1458–66.

Submitted for publication May 2, 2000. Accepted in revised form August 15, 2000.